BIOCHEMISTRY
including biophysical chemistry & molecular biology

Article

pubs.acs.org/biochemistry

Mechanism of the Enzymatic Synthesis of 4-(Hydroxymethyl)-2-furancarboxaldehyde-phosphate (4-HFC-P) from Glyceraldehyde-3-phosphate Catalyzed by 4-HFC-P Synthase

Yu Wang, Michael K. Jones, Huimin Xu, W. Keith Ray, and Robert H. White*

Department of Biochemistry, Virginia Polytechnic Institute and State University, Blacksburg, Virginia 24061, United States

Supporting Information

ABSTRACT: A single enzyme, 4-(hydroxymethyl)-2-furancarboxaldehyde-phosphate synthase (MfnB), from the methanogen *Methanocaldococcus jannaschii* catalyzed at least 10 separate chemical reactions in converting two molecules of glyceraldehyde-3-P (GA-3-P) to 4-(hydroxymethyl)-2-furancarboxaldehyde-P (4-HFC-P), the first discrete intermediate in the biosynthetic pathway to the furan moiety of the coenzyme methanofuran. Here we describe the biochemical characterization of the recombinantly expressed MfnB to understand its catalytic mechanism. Site-directed mutagenesis showed that the strictly conserved residues (Asp25, Lys27, Lys85, and Asp151) around the active site are all essential for enzyme catalysis. Matrix-assisted laser desorption/ionization analysis of peptide fragments of MfnB incubated with GA-3-P followed by $NaBH_4$ reduction and trypsin digestion identified a peptide with a mass/charge ratio of 1668.8 *m/z* present only in the D25N, D151N, and K155R mutants, which is consistent with Lys27 having increased by a mass of 58 *m/z*, indicating that Lys27 forms a Schiff base with a methylglyoxal-like intermediate. In addition, incubation of MfnB with GA-3-P in the presence of deuterated water or incubation of MfnB with C-2 deuterated GA-3-P showed essentially no deuterium incorporated into the 4-HFC-P. Combined with structural analysis and molecular docking, we predict the potential binding sites for two GA-3P molecules in the active site. On the basis of our observations, a possible catalytic mechanism of MfnB is proposed in this study. A phosphate elimination reaction and a triose phosphate isomerase-like reaction occur at the GA-3-P binding site I and II, respectively, prior to the aldol condensation between the enzyme-bound enol form of methylglyoxal and dihydroxyacetone phosphate (DHAP), after which the catalytic cycle is completed by a cyclization and two dehydration reactions assisted by several general acids/bases at the same active site.

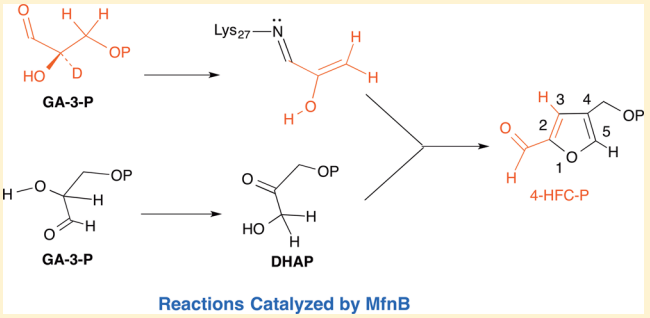

Reactions Catalyzed by MfnB

Methanofuran is the first in a series of coenzymes involved in the biochemical reduction of carbon dioxide to methane.[1−3] This process, known as methanogenesis, is carried out only by the methanogenic archaea that produce more than 400 million tons of methane each year as an essential part of the global carbon cycle.[4] The chemical structure of methanofuran varies among different methanogens;[5] each currently known methanofuran molecule contains the basic core structure of 4-[*N*-(γ-L-glutamyl-γ-L-glutamyl)-*p*-(β-aminoethyl)phenoxymethyl]-2-(aminomethyl)furan (APMF-$(Glu)_2$), but different analogues have different attached side chains. Recently, our laboratory identified new methanofuran structures in *Methanocaldococcus jannaschii*, which contains a long γ-glutamyl tail with 7−12 γ-linked glutamates[6] (Figure 1). Although the function of methanofuran has been known for many years, its biosynthetic pathway has not been fully elucidated.

Recently, using a combination of comparative genomics analyses and an *in vitro* assay,[7] we identified 4-(hydroxymethyl)-2-furancarboxaldehyde-phosphate synthase (MfnB) as the enzyme catalyzing the formation of 4-(hydroxymethyl)-2-furancarboxaldehyde-P (4-HFC-P) from glyceraldehyde-3-P (GA-3-P). 4-HFC-P is then transaminated by 4-HFC-P:alanine aminotransferase (MfnC) to produce 5-(aminomethyl)-3-furanmethanol phosphate (F1-P), the precursor for the furan moiety in methanofuran (Figure 1).[7] We previously demonstrated that the MJ0050 gene encodes a tyrosine decarboxylase that produces tyramine from tyrosine.[8] A tyramine-glutamate ligase (the gene product of MJ0815) catalyzes the ATP-dependent addition of one glutamate to tyramine via a γ-linked amide bond[9] (Figure 1). These results led us to propose the remaining steps of methanofuran biosynthesis to be as shown in Figure 1.

MJ1099 was originally annotated in the database as a hypothetical enzyme containing the DUF556 domain. Its homologues are distributed in all methanogens and some methylotrophic bacteria, all of which require methanofuran and methanopterin as coenzymes.[10,11] PSI-blast analysis indicated

Received: February 20, 2015
Revised: April 22, 2015
Published: April 23, 2015

DOI: 10.1021/acs.biochem.5b00176
Biochemistry 2015, 54, 2997−3008

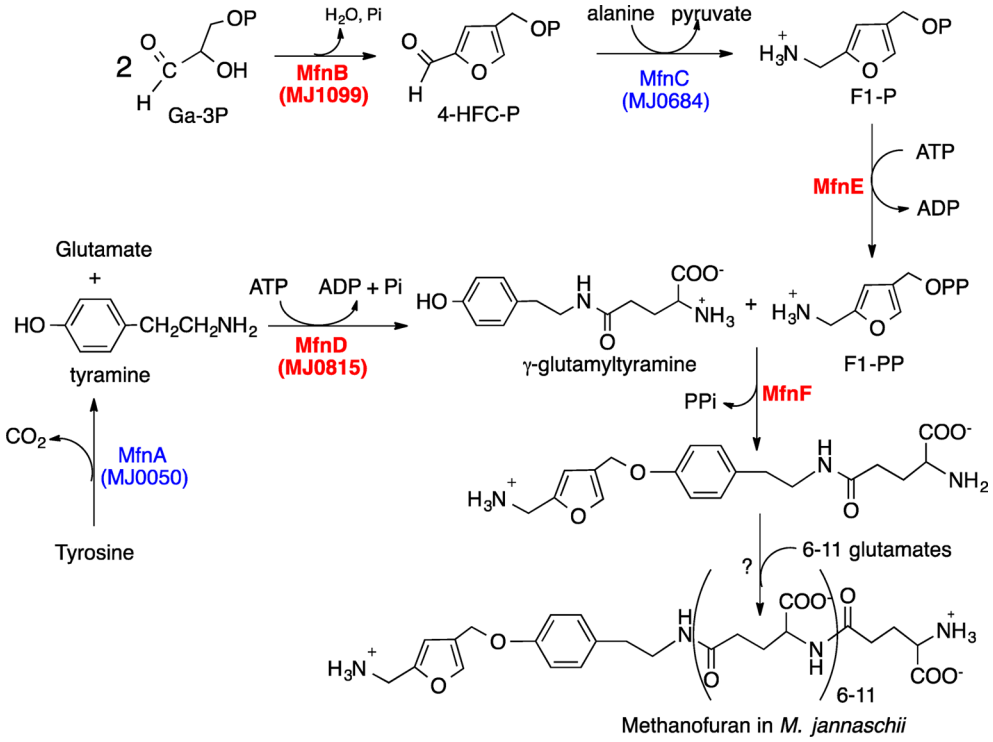

Figure 1. Proposed biosynthetic pathway of methanofuran in *M. jannaschii*.

that the MJ1099 gene product contained a class I aldolase domain (from residues 10 to 106). The recently solved crystal structure of MfnB from *M. jannaschii*[12] exhibits a typical α/β TIM barrel fold,[13−18] which is commonly seen within the class I aldolase enzymes. Multiple lysine and aspartic acid residues commonly occur in the active site of class I aldolase enzymes, where the formation of a Schiff base with the substrate is required for catalysis.[19] Sequence alignment of MfnB homologues as well as MfnB's crystal structure reveal three lysine residues and two aspartic acid residues that are strictly conserved in the putative active site, indicating that MfnB may follow the class I aldolase mechanism. However, on the basis of the structures of the substrate and product of the reaction, it is clear that additional reactions including a phosphate elimination reaction, isomerization, aldol condensation, cyclization, and dehydration would be required to operate in a single active site.[7]

To understand the mechanism of MfnB, we have biochemically interrogated the reaction catalyzed by the recombinantly expressed *M. jannaschii* MfnB. We describe a kinetic study and a site-directed mutagenesis study of five conserved amino acid residues to determine their functional roles in the mechanism of this enzyme. In addition, we used chemical trapping combined with matrix-assisted laser desorption/ionization (MALDI) analysis to identify the enzyme-bound intermediates, which provides an important perspective for a possible catalytic mechanism. By molecular docking two GA-3-P molecules to the MfnB active site, we predicted two possible binding pockets. Combined with the comparison of the structures of other class I aldolases, triose phosphate isomerase (TIM), and methylglyoxal synthase (MGS) with MfnB, a catalytic mechanism for MfnB is proposed in this study.

MATERIALS AND METHODS

Chemicals. All reagents were purchased from Sigma-Aldrich unless otherwise specified.

Synthesis of 4-HFC and 4-HFC-P. 4-(Hydroxymethyl)-2-furancarboxaldehyde (4-HFC) was prepared by treatment of dihydroxyacetone with a series of ion exchange resins as described in example 3 from United States Patent 8455668 B2. Thin layer chromatography (TLC) analysis of the product using methyl acetate as the solvent showed that the resulting 4-HFC had an R_f of 0.49 and contained less than 5% of the 5-isomer, 5-(hydroxymethyl)-2-furancarboxaldehyde (5-HFC), which had an R_f of 0.56 in this solvent. ^{1}H NMR (400 Mz, D_2O) δ 9.297 (1H, d, $J_{CHO\rightarrow H\text{-}5}$ = 0.8 Hz, CHO), 7.713 (1H, pentet, $J_{H\text{-}5\rightarrow CHO}$ = 0.8 Hz, $J_{H\text{-}5\rightarrow CH_2}$ = 0.8 Hz, $J_{H\text{-}5\rightarrow H\text{-}3}$ = 0.8 Hz, H-5) 4.4025 (2H, m, CH_2). Assignments were confirmed with COSY and HSQC.

To synthesize 4-HFC-P, 4-HFC (43 mg, 0.34 mmol) was dissolved in 1 mL of acetonitrile to which 60 μL of trichloroacetonitrile (60 μL, 0.6 mmol) and tetrabutylammonium phosphate (150 mg, 0.44 mmol) was dissolved. This procedure was patterned after a previously described method.[20] After 4 h (at room temperature), solvent was evaporated with a stream of nitrogen gas, and the sample was mixed with 1 mL of water and cooled overnight at 3 °C. The resulting trichloroacetoamide crystals were separated by filtration, and the resulting solution was passed through a Dowex 50 NH_4^+ column (0.5 × 2 cm) to remove the tetrabutylammonium cation. Portions of the resulting solution were purified by preparative thin layer chromatography (TLC) using the acetonitrile−water−formic acid (88%) solvent system, (19:2:1 vol/vol/vol). The desired product had an R_f of 0.58, and the position of the compound was identified by its 280 nm UV absorbance. The band having the 280 nm UV absorbance was removed from the TLC plate, and 4-HFC-P was eluted with the

DOI: 10.1021/acs.biochem.5b00176
Biochemistry 2015, 54, 2997−3008

TLC solvent. The solvent was evaporated, and the sample was dissolved in water. Analysis of the sample by HPLC[7] showed that it was chromatographically pure and eluted as a single peak with an absorbance maximum at 280 nm. Treatment of the sample with phosphatase generated 4-HFC that eluted with a longer retention position but having the same absorbance spectrum.[7]

Cloning and Expression of the *M. jannaschii* MJ1099 and Generation of *M. jannaschii* MJ1099 Mutants. The *M. jannaschii* gene at locus MJ1099 (UniProt Q58499) was recombinantly produced and expressed as previously described.[7] The Quick-Change TM site-directed mutagenesis kit (Stratagene) was used to construct MJ1099 mutants according to the manufacturer's instructions using template pMJ1099. Primers used for the mutants are listed in Table S1, Supporting Information. The sequences of plasmids carrying the MJ1099 gene and its mutations were confirmed by sequencing the inserted gene (DNA Facility of Iowa University).

Purification and Identification of Recombinant *M. jannaschii* MfnB. The gene products of MJ1099 and its variants were purified as previously described.[7] Protein concentration was determined by Bradford analysis.[21] The identity of the purified enzyme was verified by MALDI mass spectral analysis of the excised protein band from the polyacrylamide gel, following in-gel trypsin digestion, using a 4800 MALDI TOF/TOF mass spectrometer (Applied Biosystems) as previously described.[22]

Standard Assays of MfnB. In a 100 μL reaction volume, 5 μg of enzyme (MfnB) was incubated with 1 mM GA-3-P in 50 mM HEPES/K^+ buffer at pH 7.0 at 70 °C for 20 min. Product formation was analyzed by HPLC as previously described.[7] The initial rate of 4-HFC-P formation was measured at 280 nm using a Shimadzu UV-1601 spectrophotometer equipped with a cell temperature controller. The molar absorptivity of 4-HFC-P (ε_{280} = 15 900 M^{-1} cm^{-1}) was obtained by the following procedure. The ^{1}H NMR spectrum of a pure sample 4-HFC in deuterated chloroform ($CDCl_3$) containing a known amount of tetramethylsilane (TMS) was recorded and from the ratios of the proton intensities of the 4-HFC to the TMS intensities the concentration in the 4-HFC was calculated. The sample was then evaporated and placed in the same volume of methanol. A portion of this solution was diluted into water, and the absorbance spectrum was recorded and the molar absorptivity was calculated. Hydrolysis of the phosphate in a 4-HFC-P sample did not alter the absorbance spectra, indicating that 4-HFC had the same molar absorptivity as 4-HFC-P.

To test the ability of MfnB to catalyze the reverse reaction, the production of GA-3-P from 4-HFC-P, a 100 μL reaction volume containing 300 μg of enzyme (MfnB) was incubated with 250 μM synthetic 4-HFC-P in 50 mM HEPES/K^+ buffer at pH 7.0 at 70 °C for 60 min. The resulting mixture was then assayed for the production of GA-3-P and DHAP. To detect the generation of GA-3-P, the entire assay mixture (100 μL) was transferred to a 1000 μL assay system containing 1 mM NAD^+ and 0.02 mg/mL D-glyceraldehyde-3-phosphate dehydrogenase in 15 mM sodium pyrophosphate/30 mM sodium arsenate, pH 8.5, at room temperature. NADH formation was followed at 340 nm to monitor the formation of GA-3-P. To detect the formation of DHAP, another assay mixture (100 μL) was transferred to a 1000 μL assay system including 1 unit/mL glycerol-3-phosphate dehydrogenase in 0.1 M triethanolamine buffer, pH 7.9, in the presence of 0.54 mM NADH. The change at 340 nm was used to monitor the formation of DHAP.

Substrate Specificity. Under the standard enzymatic assay conditions, specific activities were measured using 1 mM of the following possible substrates: pyruvate, methylglyoxal (MG), phosphoenolpyruvate (PEP), oxaloacetic acid (OAA), dihydroxyacetone (DHA), and dihydroxyacetone-phosphate (DHAP) separately and in different combinations in place of GA-3-P. To test if MfnB uses the D-isomer of GA-3-P as the substrate, MfnB was incubated with the D-GA-3-P produced from D-fructose-1,6-diphosphate by D-fructose-1,6-diphosphate aldolase (FBP aldolase). In a 100 μL reaction volume, 5 mM D-fructose-1,6-diphosphate was incubated with 0.8 U aldolase from rabbit muscle (4 U/mL) in 50 mM HEPES buffer, pH 7.0, at room temperature for 20 min. Then, a 50 μL reaction mixture was transferred and incubated with 60 μg of MfnB in 50 mM 4-(2-hydroxyethyl)-1-piperazineethanesulfonic acid (HEPES) buffer, pH 7.0, at 70 °C for 20 min. Then the samples were analyzed by HPLC as previously described.[7]

pH and Metal-Dependence of MfnB. To investigate the influence of pH on catalytic ability, the specific activity at varying pHs was measured. The standard enzymatic assay was conducted in 25 mM citrate (pH 4.0−6.0), 25 mM 4-morpholineethanesulfonic acid (MES) (pH 6.0−7.0), and 25 mM tricine/3-(cyclohexylamino)1-propanesulfonic acid (CAPS)/*N*-[tris(hydroxymethyl)methyl]2-amionoethanesulfonic acid (TES) buffer from pH 6.7 to 11.5 for 20 min at 70 °C. To test the influence of metal ions on MfnB activity, the standard enzymatic assay was carried out and included 1 mM of one of the following cations: Mg^{2+}, Mn^{2+}, Ni^{2+}, Co^{2+}, Cu^{2+}, Zn^{2+}, K^+, or 10 mM EDTA.

Steady-State Kinetic Study. The apparent kinetic parameters were determined at 70 °C by measuring 4-HFC-P formation catalyzed by MfnB in a 100 μL reaction volume including 4 μg of wild-type MfnB or its variants in 50 mM HEPES/K^+ buffer, pH 7.0, with various concentrations of GA-3-P ranging from 0.01 to 1 mM. The initial rate of formation of 4-HFC-P was measured at 280 nm using a Shimadzu UV-1601 spectrophotometer equipped with a cell temperature controller. The apparent kinetic constants were calculated by fitting the data to the Michaelis equation using Prism 5.0c.

Incubation of MfnB with GA-3-P in the Presence of Deuterated Water. A 1000 μL portion of 50 mM MES buffer pH 7.0 was evaporated to dryness under N_2, and the water was replaced with 1000 μL of deuterated water (99.8% ^{2}H). Using this buffer, the standard assay was performed at 70 °C for 30 min, and then the reaction mixture was treated with 1 μL phosphatase (0.2 U/L) to generate 4-HFC from the 4-HFC-P. The resulting 4-HFC was assayed by LC-ESI-MS for the presence of deuterium using the $(M + H)^+$ = 127 m/z ion to measure the deuterium incorporation.

Incubation of MfnB with a Deuterated GA-3-P. A mixture of deuterated GA-3-P/DHAP was prepared by exchange labeling of DHAP with triose phosphate isomerase (TIM) (Sigma-Aldrich T6258) in D_2O. Thus, a 110 μL reaction volume containing 10 mM DHAP in 50 mM MES buffer in D_2O was incubated with 0.3 U of TIM at 25 °C for 20 min. To 20 μL of this incubation mixture was dissolved ~0.1 mg of $NaBH_4$. After 20 min at 25 °C, 1 μL of acetic acid was added leading to the generation of hydrogen gas. The resulting sample contained α-glycerol-phosphate that was produced from the reduction of both [1(*R*)-^{2}H]-DHAP and [2(*R*)-^{2}H]-GA-3-P that were present in the incubation mixture. After evaporation of the water with a stream of nitrogen gas, the sample was repeatedly dissolved in 200 μL of methanol and evaporated to

DOI: 10.1021/acs.biochem.5b00176
Biochemistry 2015, 54, 2997−3008

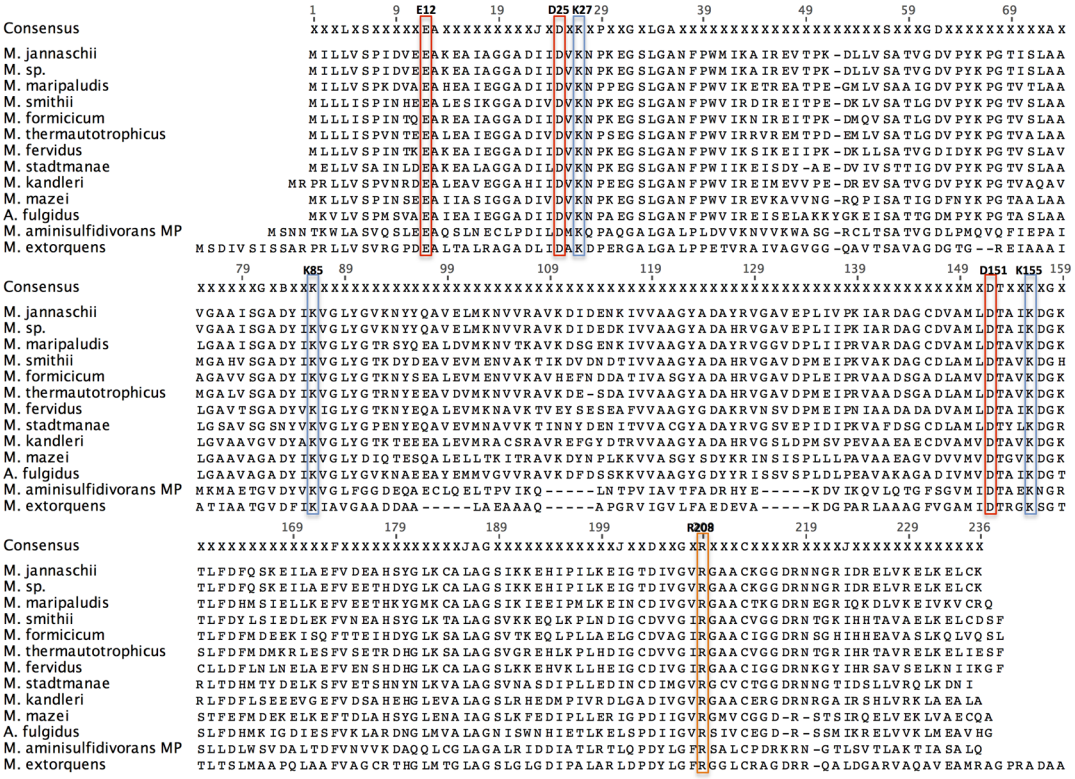

Figure 2. Multiple sequence alignment of MfnB homologues. The accession numbers of each sequence are as follows: *M. jannaschii*, Q58499; *Methanocaldococcus sp.*, A0A076LJA6; *Methanococcus maripaludis*, A6VK15; *Methanobrevibacter smithii*, R7PQR7; *Methanobacterium formicicum*, A0A090JX40; *Methanothermobacter thermautotrophicus*, T2GHG3; *Methanothermus fervidus*, E3GXG6; *Methanosphaera stadtmanae*, Q2NH72; *Methanopyrus kandleri*, Q8TUZ9; *Methanosarcina mazei*, M1Q8N3; *Archaeoglobus fulgidus*, A0A075WIX5; *Methylophaga aminisulfidivorans*, F5SZ22; *Methylobacterium extorquens*, A9W3T7.

remove the borate as the trimethyl ester. The final solid was dissolved in 200 μL of water and passed thought a Dowex-50 H^+ column. The recovered sample was evaporated to dryness and dissolved in 60 μL of water for ESI-mass spectral analysis of the content of deuterium α-glycerol-phosphate ($(M - H)^-$ = 172 m/z).

To another 50 μL TIM-catalyzed reaction mixture from above was added 28 μg of MfnB and incubated at 70 °C for 10 min, and then the reaction mixture was treated by phosphatase to generate 4-HFC from the 4-HFC-P. The resulting 4-HFC was assayed by LC-ESI-MS for the presence of deuterium using the $(M + H)^+$ = 127 m/z ion to measure the deuterium incorporation.

Chemical Trapping and Identification of the Schiff Base Intermediate. Purified wild-type MfnB and five variants (400−600 μg/mL) were incubated with 3.3 mM GA-3-P (in a 40 μL reaction volume) at 70 °C for 20 min in 25 mM MES buffer, pH 7.0. The resulting samples were then treated with ∼14 mM sodium borohydride ($NaBH_4$) at room temperature for 30 min. The salts were removed by dialysis against 25 mM ammonium acetate, pH 7.1, for 1.5 h. Protein samples were then acidified by bringing the final trifluoroacetic acid (TFA) concentration to 0.1% (v/v) using a 5% (v/v) stock, and the pH was further adjusted to below 3 using 98% (v/v) formic acid. The samples were then desalted utilizing 100 μL of OMIX C4 solid-phase extraction pipet tips (Varian) following the manufacturer's instructions. The desalted protein solutions were dried using a centrifugal vacuum concentrator and resolubilized in 200 μL freshly prepared 100 mM ammonium bicarbonate. Four micrograms of sequencing-grade trypsin (Sigma) were added to each sample, and the digestions were incubated overnight at 37 °C. The following day, 1.5 μL of each digestion was spotted onto a stainless steel MALDI target plate (AB Sciex) and allowed to air-dry. The MALDI plate spots were then overlaid with 1 μL of α-cyano-4-hydroxycinnamic acid matrix solution (4 mg/mL in 50:50 LC-MS grade water: LC-MS grade acetonitrile containing 0.1% TFA and 10 mM ammonium chloride). Mass spectra were obtained using a 4800 MALDI Tof/Tof (AB Sciex) after calibration of the instrument utilizing a six peptide mixture, summing the results from 1000 laser shots covering the m/z range of 800−4000. Selected peptides were fragmented by collision-induced dissociation (CID) to confirm their sequences.

Molecular Docking of GA-3-P into the Active Site. The GA-3-P structure was obtained from the RCSB Protein Data Bank (PDB: 1UOD). The X-ray crystal structure of MfnB from *M. jannaschii* was deposited in the PDB database as PDB 4U9P.[12] The protein and substrate files for molecular docking were prepared using AutoDock Tools 1.5.6.[23] AutoDock Vina[24] built in Chimera[25] was used to perform the molecular docking of GA-3-P into MfnB. The parameters of molecular docking for one molecule of GA-3-P were a box size of 20 Å × 25 Å × 30 Å that was centered within the coordinates of (−25, 20, −20). The parameters of molecular docking for the second molecule of GA-3-P were a box size of 15 Å × 15 Å × 8 Å that was centered within the coordinates of (13, 17, 6). The models we chose considered both energy and reasonable orientation and conformation.

DOI: 10.1021/acs.biochem.5b00176
Biochemistry 2015, 54, 2997−3008

RESULTS

Recombinant Expression, Purification, and Analysis of the Gene Products of MJ1099 and Its Variants. The gene MJ1099 was cloned, and the gene product was overexpressed in *E. coli* as previously described.[7] Wild-type MfnB and its five variants were all found to possess high thermal stability following heating at 80 °C for 10 min and thus were purified by heating the *E. coli* cell extracts to 80 °C followed by purification of the MfnB by anion exchange chromatography.[7] The wild-type enzyme, as well as each of five variants, eluted as a single peak centered at 0.40 M NaCl. Each purified protein migrated as a single band with an apparent molecular mass of 25 kDa and was greater than 95% pure as evaluated by SDS-PAGE. The identity of the purified protein, as well as the presence of the expected mutation, was confirmed by MALDI-MS/MS analysis of the tryptic-digested protein bands from the SDS gel as previously described.[22]

MfnB Catalyzed Reactions. The gene product of MJ1099 (MfnB) has been shown to catalyze the formation of 4-HFC-P from GA-3-P.[7] MfnB incubated with pyruvate, MG, PEP, OAA, DHA, and DHAP, separately and in combination, showed no expected products, indicating that GA-3-P is the sole substrate for MfnB. In addition, MfnB could use the D-isomer of GA-3-P as the substrate, which was generated from D-fructose-1,6-diphosphate by FBP aldolase. A possible mechanism is proposed that one molecule of D-GA-3-P is likely converted to enzyme-bound MG or enol form of MG as a part of Schiff base that then undergoes an aldol condensation with DHAP formed from the second molecule of D-GA-3-P. The condensation product then undergoes several additional steps to form the final product 4-HFC-P. In addition, incubation of the enzyme with various concentrations of DHAP along with GA-3-P had no influence on the formation of 4-HFC-P. The formation of 4-HFC-P from two molecules of GA-3-P must proceed through an isomerization reaction where one molecule of GA-3-P is converted into DHAP in the active site to condense with the enzyme-bound MG or the enol form of MG as a part of Schiff base generated from the other molecule of GA-3-P. This isomerization reaction must occur in the active site without release of DHAP since no DHAP was detected in the reaction mixture during catalysis. In addition, no GA-3-P or DHAP was detected when MfnB was incubated with 4-HFC-P, indicating that the MfnB catalyzed reaction is irreversible.

One of the Steps in the MfnB Catalyzed Reaction Is Analogous to that in Class I Aldolases. Aldolases are generally divided into two classes based on their mechanism.[26] Class I enzymes utilize the formation of a Schiff base between the carbonyl-group of the substrate and the amino group of a conserved lysine residue in the active site to generate an iminium intermediate.[19] In contrast, the mechanism of the class II enzymes utilizes Zn(II) as a Lewis acid and an active site base for proton abstraction and formation of the enol intermediate.[27] A PSI-BLAST analysis[28] indicated that MfnB belongs to the COG1891 superfamily that contains a class I aldolase domain (from residues 10−106) and had nonspecific hits to the protein family COG0274, which encodes deoxyribose-phosphate aldolase (a class I aldolase). Indeed, sequence alignment of MfnB and its homologues showed that three lysine residues (Lys27, Lys85, and Lys155 in *M. jannaschii* MfnB) are strictly conserved (Figure 2), with one possibly being involved in the formation of the Schiff base during catalysis. Indeed, the addition of a whole series of likely metal ions or EDTA had no influence on MfnB activity, further indicating that MfnB likely employs a class I aldolase mechanism for the aldol condensation step. In addition, class I aldolases catalyzing the cleavage/condensation of a carbon−carbon bond usually follow a general acid/base mechanism. Therefore, we evaluated the influence of pH on MfnB activity. The pH profile exhibited a bell-shaped dependence on pH with the optimum around pH 7.0 (Figure 3). Notably, although one of steps in MfnB requires

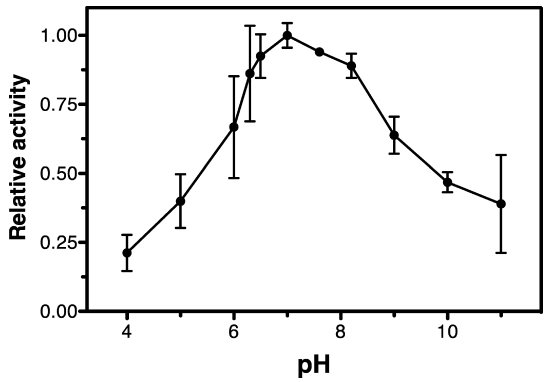

Figure 3. pH profile of MfnB.

a Schiff base, the scenario of the aldol condensation is distinctive since the Schiff base is likely formed at C-1 of GA-3-P, but C-3 undergoes the aldol condensation reaction, unlike other class I aldolases.

Incubation of MfnB with GA-3-P in the Presence of Deuterated Water. When the enzyme was incubated with GA-3-P in the presence of 99% D_2O, no deuterium was incorporated into the 4-HFC, as measured by LC-ESI-MS. Analysis of an unlabeled synthetic 4-HFC mass spectrum showed the measured intensities ratio of $(M + 1 + H)^+/(M + H)^+$ to be 0.14, whereas the sample produced by the enzyme in the presence of 99% D_2O showed this ratio as 0.16. This result showed that <2% of product 4-HFC had incorporated deuterium, indicating that either no reaction intermediate had undergone a C−H exchange with the D_2O, or that the solvent-derived deuterium was lost in a subsequent step.

Incubation of MfnB with Deuterated GA-3-P. It is well-known that TIM readily exchanges the C-1 *pro-R* hydrogen in DHAP and the C-2 hydrogen in GA-3-P with solvent during its isomerization reaction.[29] The C-2 deuterated GA-3-P was prepared by exchange labeling of DHAP with triose phosphate isomerase (TIM). After reduction of GA-3-P/DHAP to α-glycerol-phosphate, it was established that the α-glycerol-phosphate was labeled to an extent of 96% with one deuterium, indicating that the deuterated GA-3-P/DHAP mixture was prepared successfully. LC-MS analysis of 4-HFC generated from the deuterated GA-3-P incubated with MfnB followed by phosphatase treatment showed the measured intensities ratio of $(M + 1 + H)^+/(M + H)^+$ to be 0.13, compared to the intensities ratio (0.14) from an unlabeled synthetic 4-HFC, clearly showing no incorporation of deuterium in 4-HFC from deuterated GA-3-P.

Steady-State Kinetic Study of MfnB. Steady-state kinetic parameters were determined by monitoring the absorbance change at 280 nm for 4-HFC-P formation. A turnover number of k_{cat} = 0.026 ± 0.002 s^{-1} and a K_M = 35 ± 10 μM were obtained by fitting the Michaelis equation. The low turnover

DOI: 10.1021/acs.biochem.5b00176
Biochemistry 2015, 54, 2997−3008

number for MfnB possibly reflected the rate-limiting step as occurring at other steps instead of the aldol condensation step.

Effect of Substituting the Conserved Residues on MfnB Enzymatic Activity. Sequence alignment of MfnB and its homologues (COG1891 family members) showed that three lysine residues (Lys27, Lys85, and Lys155) are strictly conserved (Figure 2); at least one of them should be involved in the formation of the Schiff base during catalysis. In addition, two aspartic acid residues (Asp25 and Asp151) are also strictly conserved in the COG1891 family. To evaluate the function of these conserved residues, we selectively generated five variants (K27R, K85R, K155R, D25N, D151N) by site-directed mutagenesis. Single substitutions of Asp25, Lys27, Lys85, or Asp151 caused the complete inactivation of MfnB (Table 1). Since all variants possess high thermal stability following heating at 80 °C for 10 min and the catalytic intermediate could be trapped and detected (see below) as well, we assume that the loss of activities for those variants (K27R, K85R, D25N, D151N) is not due to misfolding, suggesting that their roles in catalysis are essential. In contrast, replacing the strictly conserved Lys155 by arginine caused subtle changes in the kinetic parameters; its k_{cat}/K_M was comparable to the wild-type, indicating that either Lys155 plays only a minor role in catalysis and substrate binding or the conservation of positive charge was all that was required for an amino acid at this position in the sequence.

Table 1. Steady-State Kinetic Parameters of *M. jannaschii* MfnB and Its Variants

	kinetic parameters at 70 °C		
	k_{cat} (s^{-1})	K_M (μM)	k_{cat}/K_M (M^{-1} s^{-1})
wild-type	0.026 ± 0.002	35 ± 10	7.4×10^2
D25N	ND[a]	ND	ND
K27R	ND	ND	ND
K85R	ND	ND	ND
D151N	ND	ND	ND
K155R	0.022 ± 0.002	48 ± 10	4.6×10^2

[a]Not detected.

Identifying the Schiff Base-Forming Lysine and the Chemical Nature of the Involved Substrate. To identify the catalytically essential Schiff base in MfnB, $NaBH_4$ was used to reduce a mixture of MfnB (either wild type or one of the five variants) and GA-3-P. The resulting proteins were then digested by trypsin. MALDI analysis of the resulting peptides identified a peptide with a mass charge ratio of 1668.8 m/z that was present only in the D25N, D151N, and K155R samples. The absence of this modified peptide in K27R, K85R can be explained by their inabilities to produce the Schiff base and the absence of this modification in the wild type is possibly due to a rapid turnover of this intermediate to product. This peptide is consistent with the peptide residues 15−30 (EAIAGGADII-DVK*NPK) where the starred lysine 27 was observed with an increased mass of 58 m/z, that could be either a 1-amino-2-propanol or a 2-amino-1-propanol derivative. The mass spectral data do not distinguish between these structures. However, considering that the produced 4-HFC had no incorporated deuterium from the labeling experiments, it most likely that a 1-amino-2-propanol derivative is attached to Lys27 (Figure 4A). We proposed that GA-3-P is converted directly to an enol form of MG without being protonated to generate a methyl group;

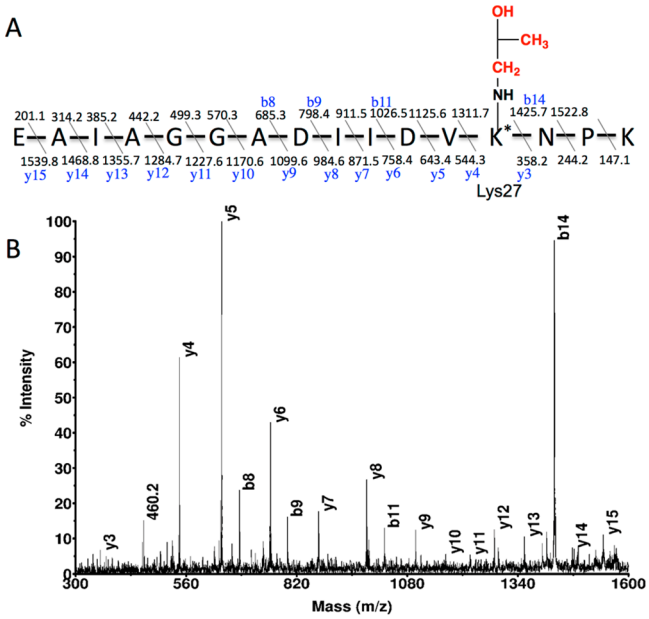

Figure 4. The Schiff base containing peptide and its CID MS. (A) The structure of the observed peptide EAIAGGADIIDVK$_{27}$NPK with a mass increase of 58 m/z. The expected fragments are numbered from b1 to b15 and from y15 to y1. The numbers reflect the observed fragments. (B) The CID MS of the 1668.8 m/z peptide present in the D25N, D151N, and K155R samples.

thus no exchange of the carbon bound hydrogen was observed. The position of modification in the sequence was also confirmed by MS/MS data (Figure 4B), indicating that Lys27 was the Schiff base-forming residue during catalysis. Screening of all the other peptide fragments failed to identify any other possible modifications on Lys27 or any modifications on other lysines.

DISCUSSION

Structural Comparison of MfnB with other Class I aldolases. Class I enzymes utilize the formation of a Schiff base between the carbonyl group of the substrate and a conserved lysine residue in the active site to generate an iminium intermediate.[19] Our results clearly showed that the aldol condensation step catalyzed by MfnB likely follows the Class I aldolase mechanism, based on the observation that MfnB activity is metal-independent and utilizes Lys27 to form a Schiff base. Although MfnB shares low similarity in sequence with other Class I aldolases (15% sequence identity with 2-deoxyribose-5-phosphate aldolase from *Rhizobium meliloti*), its crystal structure exhibits a typical α/β TIM barrel fold, which is commonly seen within Class I aldolases[12−18,30] (Figure 5). In addition, the PSI-BLAST search of MfnB showed a non-specific hit to 2-deoxyribose-5-phosphate aldolase (DERA). At the active site level, two lysines and two aspartic acids are strictly conserved in both the MfnB and DERA active site, which are essential for catalysis in both MfnB (this study) and DERA.[31]

Although the folding of MfnB shares similar features with DERA in that each subunit comprises eight/nine major α-helices and eight parallel β-strands, the orientation of the active site residues are quite different (Figure 5). In DERA, Lys167, which was proposed to be the Schiff base-forming lysine,[31−33] is located at the sixth strand (β6) of the TIM barrel. It has been reported that in almost all class I aldolases, the Schiff base-forming lysine residue is always located on the β6 strand,[31,34]

DOI: 10.1021/acs.biochem.5b00176
Biochemistry 2015, 54, 2997−3008

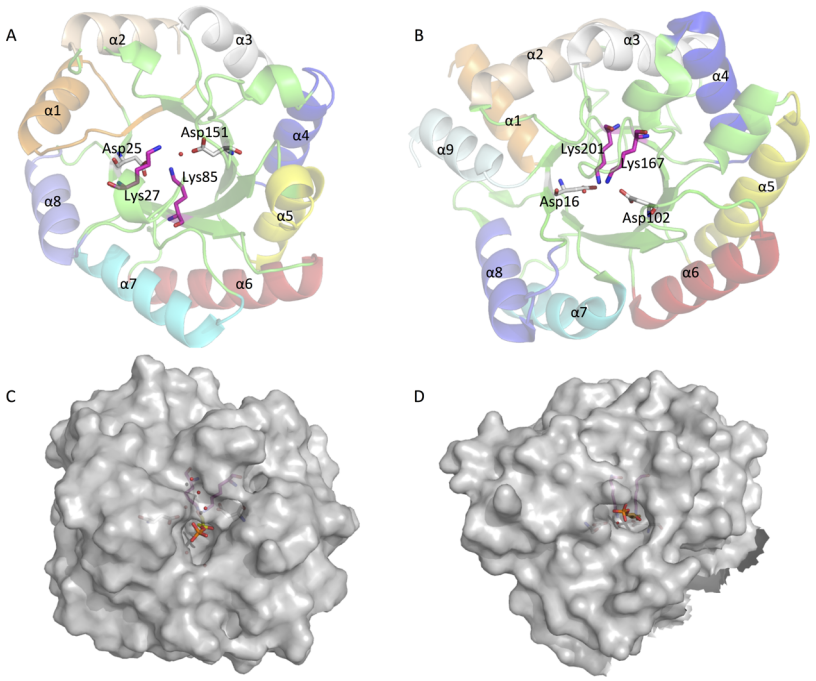

Figure 5. Comparison of the monomer structure of MfnB (PDB 4U9P) (A) and DERA (PDB 1P1X) (B); comparison of the molecule surface of MfnB with GA-3-P molecules (PDB: 1UOD) docked to the putative active site (C) and DERA with aligned 1-hydroxy-pentane-3, 4-diol-5-phosphate (PDB 1JCJ) in the active site (D).

with the exception of transaldolase B.[13] In contrast, Lys27, which is shown to be the Schiff base-forming residue in MfnB, is located on the β1 strand. Notably, in both cases, the Schiff base-forming lysine residue is solvent-accessible,[34] whereas the other essential lysine residue (Lys85 in MfnB) is buried deep within the active site (Figure 5).

The second lysine residue (Lys85) in MfnB is located 6.4 Å away from Lys27. The site-directed mutagenesis study showed that Lys85 was essential for catalysis; substitution of Lys85 resulted in failure to form the Schiff base enol of methylglyoxal on Lys27, indicating its role in abstracting the C-2 proton from the Schiff base form of GA-3-P (step 3, Figure 6). In contrast, the equivalent lysine residue, Lys201 in DERA, which is in close vicinity (3.4 Å) of the Schiff base-forming lysine (Lys167), is believed to lower the pK_a of Lys167 and raise its nucleophilicity.[19,20] In the 2-dehydro-3-deoxy-phosphogluconate (KDPG) aldolase, this second positively charged residue is replaced by arginine.[35] In rabbit aldolase A, the equivalent Lys146 has been shown to be involved in the cleavage and condensation of the C_3-C_4 bond of the fructose 1,6-bisphosphate.[36] In porphobilinogen synthase (PBGS), both lysine residues are involved in the formation of the Schiff base with two substrates.[37−42]

The existence of acidic residues is another feature of the class I aldolase active site. In FBP aldolase, the role of these residues has been described extensively.[16,43−45] Asp33 in FBP aldolase has been shown to serve as the general base leading to C−C bond cleavage, and Glu187 acts as a general acid to protonate the leaving hydroxyl group of the carbinolamine to assist Schiff base formation.[46] Therefore, Asp25 and Asp151 may possibly play similar roles as the general acid/base during catalysis. It should be noted here that D25N and D151N allow Schiff base formation but not 4-HFC-P formation.

Comparison of MfnB with Porphobilinogen Synthase (PBGS). PBGS catalyzes the first reaction in the biosynthesis of tetrapyrroles, where two molecules of δ-aminolevulinic acid asymmetrically condense to form the monopyrrole porphobilinogen. PBGS is a "hybrid" aldolase; its mechanism not only requires Schiff base formation, but also at least half of all known PBGSs contain the catalytically essential active site zinc.[47] In the course of the PBGS catalyzed reaction, at least eight bonds are made or broken in the steps of condensation, cyclization, and dehydration.[47] In terms of the mechanism, MfnB appears to share a similar chemistry with PBGS, including an asymmetric condensation of two molecules of substrate, cyclization, and dehydration to form a heterocyclic product. In contrast to PBGS, in MfnB, both substrates are converted to enzyme-bound intermediates prior to the aldol condensation steps.

Comparison of MfnB with Triose Phosphate Isomerase (TIM) and Methylglyoxal Synthase (MGS). Formation of 4-HFC-P requires that one of the steps in the mechanism of MfnB be the conversion of one molecule of GA-3-P to a Schiff base enol form of MG (step 3, Figure 6). Considering that 4-HFC-P incorporated no deuterium, it is more likely that GA-3-P was converted directly to an enol form of MG as Schiff base without being protonated since no exchange of the carbon bound hydrogen was observed (Figure 6).

Two well-studied enzymes are known to produce MG: triose phosphate isomerase (TIM)[48,49] and methylglyoxal synthase (MGS).[50] TIM catalyzes the interconversion of GA-3-P into DHAP with an undesired side reaction to produce MG,[51] and MGS converts DHAP into MG.[51] In both the TIM and MGS mechanisms, the first step for DHAP is the loss of a proton at the C3 position to form the enediolate. For the TIM-catalyzed reaction, this enediolate is then reprotonated at either the C3 or C2 position, whereas in MGS this enediolate is further collapsed to form the enol of MG and inorganic phosphate. These enzymes have different protein folds, but each has the same catalytically important conserved Glu/Asp and His

DOI: 10.1021/acs.biochem.5b00176
Biochemistry 2015, 54, 2997−3008

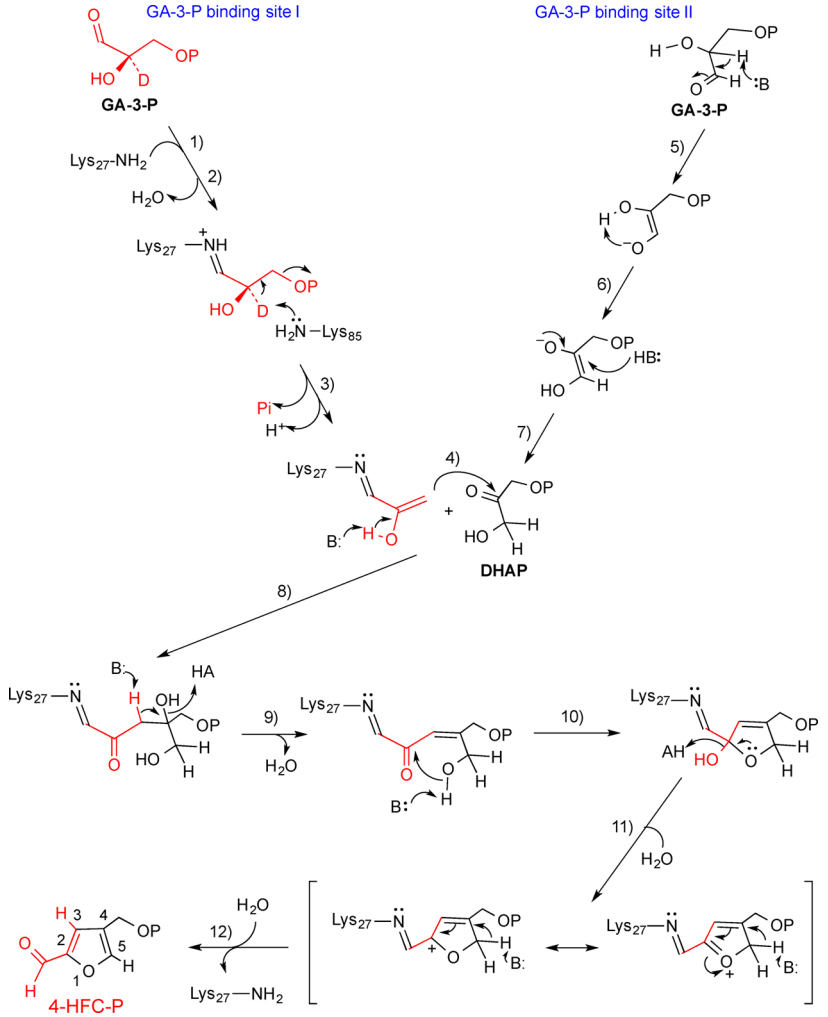

Figure 6. Scheme for the conversion of GA-3-P to 4-HFC-P catalyzed by MfnB.

residues that are located in the active sites that are enantiomorphic to each other.[50]

In addition, MGS is highly specific for using DHAP as a substrate and is not able to use either D- or L-GA-3-P as a substrate.[50] In contrast, MfnB cannot use DHAP as a substrate; instead, D-GA-3-P was shown to be the substrate. In the active site of MGS, Asp71 is the catalytic base that abstracts the proton from the C3 position of DHAP.[50] In addition, a strictly conserved histidine residue is close to the substrate.[50] However, in the active site of MfnB, there is no such histidine residue close to the putative active site. Molecular docking results (Figure 7) showed that one of the GA-3-Ps might possibly bind to a cavity composed of Ser6, Asp151, Lys155, Ala186, Gly187, Gly206, and Arg208. The aldehyde group of GA-3-P is orientated in the correct position to form a Schiff base with Lys27. At first glance, Asp151 might be acting in a similar role as Asp71 in MGS to abstract a proton from the C2 position of GA-3-P in GA-3-P binding site I. However, substitution of Asp151 to Asn had no influence on Schiff base formation. Instead, substitution of Lys85 resulted in the failure of formation of Schiff base on Lys27. This observation suggests that Lys85 is the catalytic base used to abstract the proton from the C-2 position of GA-3-P (step 3, Figure 6), which is also consistent with our observation that this hydrogen was lost during catalysis.

In the molecular docking model of MfnB, the phosphoryl-binding site is full of charged and uncharged potential hydrogen bond donors and acceptors surrounding the phosphoryl oxygens at the first GA-3-P binding site (Figure 7A), similar to the phosphoryl-binding site of MGS. A similar phosphoryl-binding site has been proposed to make the phosphoryl-moiety a better leaving group in order to facilitate phosphate elimination.[50,52,53] Furthermore, molecular docking results indicated that the positive charge on Lys155 is possibly important in stabilizing the phosphoryl-moiety of GA-3-P as a leaving group, which is also consistent with our observation that K155R retained almost full catalytic ability. This docking result was also consistent with the observation from the crystal structure of MfnB that an inorganic phosphate was observed to be bound in an almost identical location and was stabilized by the residues Lys155, Ser188, Arg208, and Arg217.[12]

In the second binding site, GA-3-P is to be converted to DHAP for a further aldol condensation reaction with the enol form of MG attached to the Lys27 Schiff base. The most widely studied enzyme converting GA-3-P to DHAP is TIM.[51] In the active site of TIM, Glu167 acts as a catalytic base to abstract a proton from the C3 of DHAP or the C2 of GA-3-P to form the enediolate intermediate;[54] Lys13 and His95 as well as Asn11 are important for electrostatic stabilization during catalysis,[55−57] and His95 is also involved in proton transfer during catalysis.[58,59] However, none of these residues appear at the

DOI: 10.1021/acs.biochem.5b00176
Biochemistry 2015, 54, 2997−3008

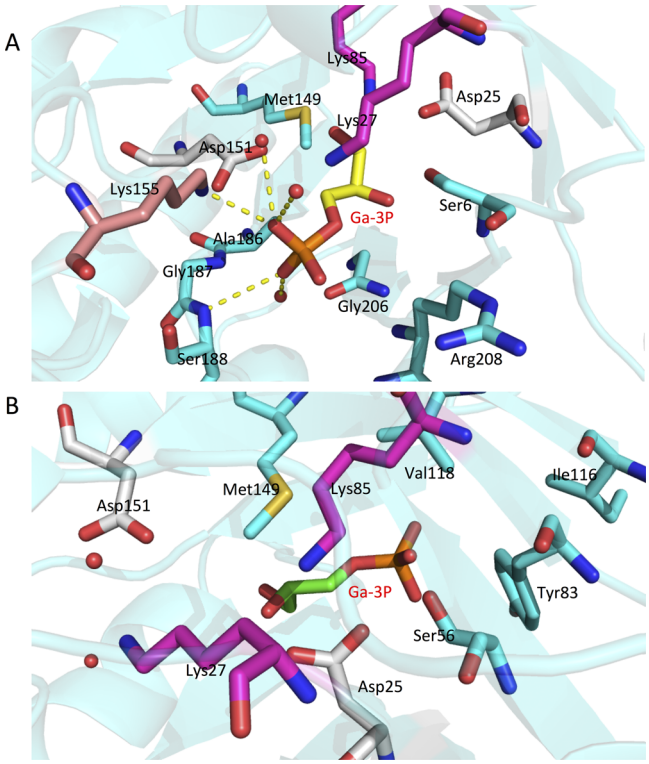

Figure 7. Molecular docking of two molecules of GA-3-P (A and B) into the active site of MfnB. In panel A, one molecule of GA-3-P (highlighted in yellow) was docked to MfnB active site, referred as GA-3-P binding site I. In panel B, the second molecule of GA-3-P (highlighted in green) was docked to MfnB active site, referred to as GA-3-P binding site II. Numbering is reflecting the *M. jannaschii* MfnB (PDB 4U9P). Red spheres represent water molecules. Dotted lines indicate inferred polar contacts. Figure was generated and presented using MacPyMOL 1.3.[69]

putative active site of MfnB. We propose that a TIM-like reaction occurs in this binding site II of MfnB; instead of a glutamate residue, Asp25 in MfnB appears to play a similar role as Glu167 in TIM, and Lys85 is possibly further used to stabilize the negatively charged intermediate. Moreover, another functionality of TIM is concerned with preventing the undesirable phosphate elimination.[60] In contrast to MGS, the hydrogen-binding network for phosphoryl oxygen in TIM is very sparse.[29,31] A mobile loop excludes bulk solvent and, thus, prevents undesirable phosphate elimination.[61] A similar loop carrying the hydrophobic residues Tyr83, Ile116, and Val 118 excludes bulk solvent to prevent phosphate elimination in MfnB, which makes the second GA-3-P site less favorable for undergoing the phosphate elimination reaction. Tyr83 is highly conserved across MfnB homologues, except in some species where it is replaced by phenylalanine (Figure 7B).

Proposed Mechanism of MfnB. On the basis of our current data, a possible catalytic mechanism of MfnB is proposed in Figure 6. In this mechanism, the enzyme active site contains two binding sites, one for each of the GA-3-Ps used in the formation of the 4-HFC-P. These will be referred to here as binding sites I and II.

In binding site I, the phosphate group is removed by an elimination reaction of the Schiff base adduct of GA-3-P. We propose that the reaction in step 1 proceeds by a Schiff base formation between the aldehyde group of GA-3-P and Lys27 to form the carbinolamine followed by the loss of water (step 2). Since no incorporation of deuterium was observed in 4-HFC when we incubated MfnB with C-2 deuterated GA-3-P, we propose that Lys85 serves as the general base to remove the C-2 proton/deuterium from the iminium form of the Schiff base, producing the enol form MG bound as the Schiff base (step 3) that then undergoes an aldol condensation (step 4) with the keto group of the DHAP (step 8) formed in binding site II. In such a mechanism, GA-3-P would be converted directly to an enol form of MG as a Schiff base without being protonated to generate a methyl group; thus no exchange of the carbon bound hydrogen was observed, consistent with our observation.

The formation of DHAP may proceed by a mechanism analogous to TIM at GA-3-P binding site II, with a general base to abstract the C2 hydrogen (step 5). Since no deuterium is incorporated into 4-HFC, then either the C-2 hydrogen is moved to C-1 with no exchange, and this hydrogen is then removed in a subsequent step or the C-2 hydrogen is completely exchanged in step 5. However, we cannot distinguish between these two options from our present data. If our mechanism for the formation of DHAP is the same or similar to TIM, then the C-1 *pro-R* hydrogen of the DHAP intermediate should be deuterated.[29] If this hydrogen is the one removed in step 12, then no deuterium would be incorporated at C-5, as is observed here. Since we do not presently know the sterochemical course of this reaction, we cannot determine which hydrogen is removed in the last hydrogen removal step. What is clear is that this would have to be the hydrogen derived from the deuterated water.

After condensation (step 8), water is eliminated (step 9), and the resulting compound is cyclized to form a 3,4-dihydrofuran by addition of the C-5 alcohol to the C-2 carbon on the Lys27 Schiff base. During steps 10−12, several general bases/acids are required to eliminate the water molecules. It is likely that Asp25, Asp151, Lys85, Ser6, and Ser56 are involved in these steps; however, we were unable to assign their function based on our current data.

The mechanism that is proposed in Figure 6 is one of the possible mechanisms that are consistent with our current data. However, in addition to the DHAP-like mechanism occurring in binding site II, another possibility that could account for lack of solvent isotope incorporation is that the enol intermediate formed in step 5 does a Michael addition reaction to the product of step 3 generated in binding site I (Supplementary Figure 1, Supporting Information). Such a mechanism would not require DHAP as an intermediate. Subsequent steps shown in Supplementary Figure 1 would then be required to generate 4-HFC-P. However, we cannot distinguish between these two options from our present data.

The Significance of MfnB as a Bioengineering Biocatalyst. Aldolases catalyzing asymmetric C−C bond formation constitute an important group of enzymes in the production of biologically important compounds. As such, aldolases have drawn much attention as sources for engineering new biocatalysts using an aldolase mechanism.[62,63] Many examples of the successful application of aldolases in chemoenzymatic synthesis have been reported, including the several sugars and their analogues;[64] new antibiotics, antimetastatic, antihyperglycemic, or immunostimulating agents;[65,66] and medicines.[67] Therefore, understanding the catalytic mechanism and structure−function relationship of MfnB might pave a way for its potential application in chemoenzymatic synthesis by engineering its substrate specificities and stereospecificity. Moreover, the MfnB-catalyzed reaction might also have

DOI: 10.1021/acs.biochem.5b00176
Biochemistry 2015, 54, 2997−3008

potential application for the synthesis of naturally occurring/complex compounds using 4-HFC-P as a precursor.[68] In addition, MfnB from *M. jannaschii* showed a high thermal stability up to 100 °C, which provides a potential application for the synthetic biology industry.

■ ASSOCIATED CONTENT

Supporting Information

An alternative possible catalytic mechanism of MfnB (Supplemental Figure 1) and primer sets for site-directed mutagenesis of MfnB (Supplemental Table S1). The Supporting Information is available free of charge on the ACS Publications website at DOI: 10.1021/acs.biochem.5b00176.

■ AUTHOR INFORMATION

Corresponding Author

*Telephone: (540) 231-6605. Fax: (540) 231-9070. E-mail: rhwhite@vt.edu.

Funding

National Science Foundation Grant MCB1120346 supported this work.

Notes

The authors declare no competing financial interest.

■ ACKNOWLEDGMENTS

The authors would like to thank Dr. Walter Niehaus for invaluable discussion and Dr. Janet Webster for editing the manuscript. We also thank Dr. W. Keith Ray and Kim C. Harich for performing the mass spectrometry experiments. The mass spectrometry resources are maintained by the Virginia Tech Mass Spectrometry Incubator, a facility operated in part through funding by the Fralin Life Science Institute at Virginia Tech and by the Agricultural Experiment Station Hatch Program (CRIS Project No. VA-135981).

■ ABBREVIATIONS

4-HFC-P, 4-(hydroxymethyl)-2-furancarboxaldehyde-P; 5-HFC, 5-(hydroxymethyl)-2-furancarboxaldehyde; APMF, 4-[[4-(2-aminoethyl)phenoxy]-methyl]-2-furan-methanamine; CAPS, 3-(cyclohexylamino)1-propanesulfonic acid; CID, collision induced dissociation; DHA, dihydroxyacetone; DHAP, dihydroxyacetone-phosphate; ESI, electrospray ionization; F1, 5-(aminomethyl)-3-furanmethanol; F1-P, 5-(aminomethyl)-3-furanmethanol-phosphate; F1-PP, 5-(aminomethyl)-3-furanmethanol-pyrophosphate; FBP aldolase, fructose-1,6,-biphosphate aldolase; GA-3-P, glyceraldehyde-3-phosphate; GC−MS, gas chromatography−mass spectrometry; HTCA, 1,3,4,6-hexanetetracarboxylic acid; MES, 4-morpholineethanesulfonic acid; MfnB, 4-HFC-P synthase; MG, methylglyoxal; MGS, methylglyoxal synthase; OAA, oxaloacetic acid; PBGS, porphobilinogen synthase; PDA, photodiode array detector; PEP, phosphoenolpyruvate; PLP, pyridoxal 5′-phosphate; TCA, trichloroacetic acid; TES, *N*-[tris(hydroxymethyl)methyl]-2-amionoethanesulfonic acid; THF, tetrahydrofuran; TIM, triose phosphate isomerase; TMS, trimethylsilyl

■ REFERENCES

(1) Ferry, J. G. (1999) Enzymology of one-carbon metabolism in methanogenic pathways. *FEMS Microbiol. Rev. 23*, 13−38.

(2) Deppenmeier, U. (2002) The unique biochemistry of methanogenesis. *Prog. Nucleic Acid Res. Mol. Biol. 71*, 223−283.

(3) Leigh, J. A., Rinehart, K. L., and Wolfe, R. S. (1984) Structure of Methanofuran, the Carbon-Dioxide Reduction Factor of *Methanobacterium thermoautotrophicum*. *J. Am. Chem. Soc. 106*, 3636−3640.

(4) Neue, H. (1993) Methane emissions from rice fields. *BioScience 43*, 466−476.

(5) White, R. H. (1988) Structural Diversity among Methanofurans from Different Methanogenic Bacteria. *J. Bacteriol. 170*, 4594−4597.

(6) Allen, K. D., and White, R. H. (2014) Identification of structurally diverse methanofuran coenzymes in methanococcales that are both *N*-formylated and *N*-acetylated. *Biochemistry 53*, 6199−6210.

(7) Miller, D., Wang, Y., Xu, H., Harich, K., and White, R. H. (2014) Biosynthesis of the 5-(Aminomethyl)-3-furanmethanol Moiety of Methanofuran. *Biochemistry 53*, 4635−4647.

(8) Kezmarsky, N. D., Xu, H., Graham, D. E., and White, R. H. (2005) Identification and characterization of a L-tyrosine decarboxylase in *Methanocaldococcus jannaschii*. *Biochim. Biophys. Acta 1722*, 175−182.

(9) Wang, Y., Xu, H., Harich, K. C., and White, R. H. (2014) Identification and Characterization of a Tyramine-Glutamate Ligase (MfnD) Involved in Methanofuran Biosynthesis. *Biochemistry 53*, 6220−6230.

(10) Chistoserdova, L., Vorholt, J. A., Thauer, R. K., and Lidstrom, M. E. (1998) C1 transfer enzymes and coenzymes linking methylotrophic bacteria and methanogenic Archaea. *Science 281*, 99−102.

(11) Pomper, B. K., and Vorholt, J. A. (2001) Characterization of the formyltransferase from *Methylobacterium extorquens* AM1. *Eur. J. Biochem. 268*, 4769−4775.

(12) Bobik, T. A., Morales, E. J., Shin, A., Cascio, D., Sawaya, M. R., Arbing, M., Yeates, T. O., and Rasche, M. E. (2014) Structure of the methanofuran/methanopterin-biosynthetic enzyme MJ1099 from *Methanocaldococcus jannaschii*. *Acta. Crystallogr., Sect. F: Struct. Biol. Commun. 70*, 1472−1479.

(13) Jia, J., Schorken, U., Lindqvist, Y., Sprenger, G. A., and Schneider, G. (1997) Crystal structure of the reduced Schiff-base intermediate complex of transaldolase B from *Escherichia coli*: mechanistic implications for class I aldolases. *Protein Sci. 6*, 119−124.

(14) Hester, G., Brenner-Holzach, O., Rossi, F. A., Struck-Donatz, M., Winterhalter, K. H., Smit, J. D., and Piontek, K. (1991) The crystal structure of fructose-1,6-bisphosphate aldolase from *Drosophila melanogaster* at 2.5 A resolution. *FEBS Lett. 292*, 237−242.

(15) Sygusch, J., Beaudry, D., and Allaire, M. (1987) Molecular architecture of rabbit skeletal muscle aldolase at 2.7-A resolution. *Proc. Natl. Acad. Sci. U. S. A. 84*, 7846−7850.

(16) Blom, N., and Sygusch, J. (1997) Product binding and role of the C-terminal region in class I D-fructose 1,6-bisphosphate aldolase. *Nat. Struct. Biol. 4*, 36−39.

(17) Izard, T., Lawrence, M. C., Malby, R. L., Lilley, G. G., and Colman, P. M. (1994) The three-dimensional structure of N-acetylneuraminate lyase from *Escherichia coli*. *Structure 2*, 361−369.

(18) Kim, H., Certa, U., Dobeli, H., Jakob, P., and Hol, W. G. (1998) Crystal structure of fructose-1,6-bisphosphate aldolase from the human malaria parasite *Plasmodium falciparum*. *Biochemistry 37*, 4388−4396.

(19) Gefflaut, T., Blonski, C., Perie, J., and Willson, M. (1995) Class I aldolases: substrate specificity, mechanism, inhibitors and structural aspects. *Prog. Biophys. Mol. Biol. 63*, 301−340.

(20) Lira, L. M., Vasilev, D., Pilli, R. A., and Wessjohann, L. A. (2013) One-pot synthesis of organophosphate monoesters from alcohols. *Tetrahedron. Lett. 54*, 1690−1692.

(21) Bradford, M. M. (1976) A rapid and sensitive method for the quantitation of microgram quantities of protein utilizing the principle of protein-dye binding. *Anal. Biochem. 72*, 248−254.

(22) Miller, D., O'Brien, K., Xu, H., and White, R. H. (2014) Identification of a 5′-deoxyadenosine deaminase in *Methanocaldococcus jannaschii* and its possible role in recycling the radical S-adenosylmethionine enzyme reaction product 5′-deoxyadenosine. *J. Bacteriol. 196*, 1064−1072.

DOI: 10.1021/acs.biochem.5b00176
Biochemistry 2015, 54, 2997−3008

(23) Morris, G. M., Huey, R., Lindstrom, W., Sanner, M. F., Belew, R. K., Goodsell, D. S., and Olson, A. J. (2009) AutoDock4 and AutoDockTools4: Automated Docking with Selective Receptor Flexibility. *J. Comput. Chem. 30*, 2785−2791.
(24) Trott, O., and Olson, A. J. (2010) AutoDock Vina: improving the speed and accuracy of docking with a new scoring function, efficient optimization, and multithreading. *J. Comput. Chem. 31*, 455−461.
(25) Pettersen, E. F., Goddard, T. D., Huang, C. C., Couch, G. S., Greenblatt, D. M., Meng, E. C., and Ferrin, T. E. (2004) UCSF Chimera–a visualization system for exploratory research and analysis. *J. Comput. Chem. 25*, 1605−1612.
(26) Allen, K. N. (1998) Reactions of enzyme-derived enamines, in *Comprehensive Biological Catalysis* (Sinnott, M., Ed.), pp 135−172, Academic Press, San Diego.
(27) Fessner, W. D., Schneider, A., Held, H., Sinerius, G., Walter, C., Hixon, M., and Schloss, J. V. (1996) The mechanism of class II, metal-dependent aldolases. *Angew. Chem., Int. Ed. 35*, 2219−2221.
(28) Altschul, S. F., Madden, T. L., Schaffer, A. A., Zhang, J., Zheng, Z., Miller, W., and Lipman, D. J. (1997) Gapped BLAST and PSI-BLAST: a new generation of protein database search programs. *Nucleic Acids Res. 25*, 3389−3402.
(29) Nickbarg, E. B., and Knowles, J. R. (1988) Triosephosphate isomerase: energetics of the reaction catalyzed by the yeast enzyme expressed in *Escherichia coli*. *Biochemistry 27*, 5939−5947.
(30) Kim, C. G., Yu, T. W., Fryhle, C. B., Handa, S., and Floss, H. G. (1998) 3-Amino-5-hydroxybenzoic acid synthase, the terminal enzyme in the formation of the precursor of mC7N units in rifamycin and related antibiotics. *J. Biol. Chem. 273*, 6030−6040.
(31) Heine, A., DeSantis, G., Luz, J. G., Mitchell, M., Wong, C. H., and Wilson, I. A. (2001) Observation of covalent intermediates in an enzyme mechanism at atomic resolution. *Science 294*, 369−374.
(32) Valentin-Hansen, P., Boetius, F., Hammer-Jespersen, K., and Svendsen, I. (1982) The primary structure of *Escherichia coli* K12 2-deoxyribose 5-phosphate aldolase. Nucleotide sequence of the deoC gene and the amino acid sequence of the enzyme. *Eur. J. Biochem. 125*, 561−566.
(33) Hoffee, P., Snyder, P., Sushak, C., and Jargiello, P. (1974) Deoxyribose-5-P aldolase: subunit structure and composition of active site lysine region. *Arch. Biochem. Biophys. 164*, 736−742.
(34) Heine, A., Luz, J. G., Wong, C. H., and Wilson, I. A. (2004) Analysis of the class I aldolase binding site architecture based on the crystal structure of 2-deoxyribose-5-phosphate aldolase at 0.99 Å resolution. *J. Mol. Biol. 343*, 1019−1034.
(35) Allard, J., Grochulski, P., and Sygusch, J. (2001) Covalent intermediate trapped in 2-keto-3-deoxy-6-phosphogluconate (KDPG) aldolase structure at 1.95-Å resolution. *Proc. Natl. Acad. Sci. U S A 98*, 3679−3684.
(36) Morris, A. J., and Tolan, D. R. (1994) Lysine-146 of rabbit muscle aldolase is essential for cleavage and condensation of the C3-C4 bond of fructose 1,6-bis(phosphate). *Biochemistry 33*, 12291−12297.
(37) Frere, F., Schubert, W. D., Stauffer, F., Frankenberg, N., Neier, R., Jahn, D., and Heinz, D. W. (2002) Structure of porphobilinogen synthase from *Pseudomonas aeruginosa* in complex with 5-fluorolevulinic acid suggests a double Schiff base mechanism. *J. Mol. Biol. 320*, 237−247.
(38) Jaffe, E. K., Kervinen, J., Martins, J., Stauffer, F., Neier, R., Wlodawer, A., and Zdanov, A. (2002) Species-specific inhibition of porphobilinogen synthase by 4-oxosebacic acid. *J. Mol. Biol. 277*, 19792−19799.
(39) Breinig, S., Kervinen, J., Stith, L., Wasson, A. S., Fairman, R., Wlodawer, A., Zdanov, A., and Jaffe, E. K. (2003) Control of tetrapyrrole biosynthesis by alternate quaternary forms of porphobilinogen synthase. *Nat. Struct. Biol. 10*, 757−763.
(40) Erskine, P. T., Coates, L., Butler, D., Youell, J. H., Brindley, A. A., Wood, S. P., Warren, M. J., Shoolingin-Jordan, P. M., and Cooper, J. B. (2003) X-ray structure of a putative reaction intermediate of 5-aminolaevulinic acid dehydratase. *Biochem. J. 373*, 733−738.
(41) Shoolingin-Jordan, P. M., Spencer, P., Sarwar, M., Erskine, P. E., Cheung, K. M., Cooper, J. B., and Norton, E. B. (2002) 5-Aminolaevulinic acid dehydratase: metals, mutants and mechanism. *Biochem. Soc. Trans. 30*, 584−590.
(42) Goodwin, C. E., and Leeper, F. J. (2003) Stereochemistry and mechanism of the conversion of 5-aminolevulinic acid into porphobilinogen catalysed by porphobilinogen synthase. *Org. Biomol. Chem. 1*, 1443−1446.
(43) Choi, K. H., Mazurkie, A. S., Morris, A. J., Utheza, D., Tolan, D. R., and Allen, K. N. (1999) Structure of a fructose-1,6-bis(phosphate) aldolase liganded to its natural substrate in a cleavage-defective mutant at 2.3 Å. *Biochemistry 38*, 12655−12664.
(44) Dalby, A., Dauter, Z., and Littlechild, J. A. (1999) Crystal structure of human muscle aldolase complexed with fructose 1,6-bisphosphate: mechanistic implications. *Protein Sci. 8*, 291−297.
(45) Littlechild, J. A., and Watson, H. C. (1993) A data-based reaction mechanism for type I fructose bisphosphate aldolase. *Trends Biochem. Sci. 18*, 36−39.
(46) Choi, K. H., Shi, J., Hopkins, C. E., Tolan, D. R., and Allen, K. N. (2001) Snapshots of catalysis: the structure of fructose-1,6-(bis)phosphate aldolase covalently bound to the substrate dihydroxyacetone phosphate. *Biochemistry 40*, 13868−13875.
(47) Jaffe, E. K. (2004) The porphobilinogen synthase catalyzed reaction mechanism. *Bioorg. Chem. 32*, 316−325.
(48) Richard, J. P. (1993) Mechanism for the formation of methylglyoxal from triosephosphates. *Biochem. Soc. Trans. 21*, 549−553.
(49) Phillips, S. A., and Thornalley, P. J. (1993) The formation of methylglyoxal from triose phosphates - Investigation using a specific assay for methylglyoxal. *Eur. J. Biochem. 212*, 101−105.
(50) Saadat, D., and Harrison, D. H. (2000) Mirroring perfection: the structure of methylglyoxal synthase complexed with the competitive inhibitor 2-phosphoglycolate. *Biochemistry 39*, 2950−2960.
(51) Wierenga, R. K., Kapetaniou, E. G., and Venkatesan, R. (2010) Triosephosphate isomerase: a highly evolved biocatalyst. *Cell. Mol. Life. Sci. 67*, 3961−3982.
(52) Cui, Q., and Karplus, M. (2003) Catalysis and specificity in enzymes: a study of triosephosphate isomerase and comparison with methyl glyoxal synthase. *Adv. Protein. Chem. 66*, 315−372.
(53) Marks, G. T., Harris, T. K., Massiah, M. A., Mildvan, A. S., and Harrison, D. H. T. (2001) Mechanistic implications of methylglyoxal synthase complexed with phosphoglycolohydroxamic acid as observed by X-ray crystallography and NMR spectroscopy. *Biochemistry 40*, 6805−6818.
(54) Campbell, I. D., Jones, R. B., Kiener, P. A., and Waley, S. G. (1979) Enzyme-substrate and enzyme-inhibitor complexes of triose phosphate isomerase studied by 31P nuclear magnetic resonance. *Biochem. J. 179*, 607−621.
(55) Kursula, I., Partanen, S., Lambeir, A. M., Antonov, D. M., Augustyns, K., and Wierenga, R. K. (2001) Structural determinants for ligand binding and catalysis of triosephosphate isomerase. *Eur. J. Biochem. 268*, 5189−5196.
(56) Lodi, P. J., Chang, L. C., Knowles, J. R., and Komives, E. A. (1994) Triosephosphate isomerase requires a positively charged active site: the role of lysine-12. *Biochemistry 33*, 2809−2814.
(57) Belasco, J. G., and Knowles, J. R. (1980) Direct observation of substrate distortion by triosephosphate isomerase using Fourier transform infrared spectroscopy. *Biochemistry 19*, 472−477.
(58) Knowles, J. R. (1991) Enzyme catalysis: not different, just better. *Nature 350*, 121−124.
(59) Bash, P. A., Field, M. J., Davenport, R. C., Petsko, G. A., Ringe, D., and Karplus, M. (1991) Computer simulation and analysis of the reaction pathway of triosephosphate isomerase. *Biochemistry 30*, 5826−5832.
(60) Richard, J. P. (1991) Kinetic parameters for the elimination reaction catalyzed by triosephosphate isomerase and an estimation of the reaction's physiological significance. *Biochemistry 30*, 4581−4585.
(61) Pompliano, D. L., Peyman, A., and Knowles, J. R. (1990) Stabilization of a reaction intermediate as a catalytic device: definition

DOI: 10.1021/acs.biochem.5b00176
Biochemistry 2015, 54, 2997−3008

of the functional role of the flexible loop in triosephosphate isomerase. *Biochemistry 29*, 3186−3194.
(62) Windle, C. L., Muller, M., Nelson, A., and Berry, A. (2014) Engineering aldolases as biocatalysts. *Curr. Opin. Chem. Biol. 19*, 25−33.
(63) Samland, A. K., and Sprenger, G. A. (2006) Microbial aldolases as C-C bonding enzymes-unknown treasures and new developments. *Appl. Microbiol. Biotechnol. 71*, 253−264.
(64) Schuster, M., He, W. F., and Blechert, S. (2001) Chemical-enzymatic synthesis of azasugar phosphonic acids as glycosyl phosphate surrogates. *Tetrahedron. Lett. 42*, 2289−2291.
(65) Espelt, L., Bujons, J., Parella, T., Calveras, J., Joglar, J., Delgado, A., and Clapes, P. (2005) Aldol additions of dihydroxyacetone phosphate to N-Cbz-amino aldehydes catalyzed by L-fuculose-1-phosphate aldolase in emulsion systems: inversion of stereoselectivity as a function of the acceptor aldehyde. *Chemistry 11*, 1392−1401.
(66) Espelt, L., Parella, T., Bujons, J., Solans, C., Joglar, J., Delgado, A., and Clapes, P. (2003) Stereoselective aldol additions catalyzed by dihydroxyacetone phosphate-dependent aldolases in emulsion systems: preparation and structural characterization of linear and cyclic iminopolyols from aminoaldehydes. *Chemistry 9*, 4887−4899.
(67) DeSantis, G., Liu, J., Clark, D. P., Heine, A., Wilson, I. A., and Wong, C. H. (2003) Structure-based mutagenesis approaches toward expanding the substrate specificity of D-2-deoxyribose-5-phosphate aldolase. *Bioorg. Med. Chem. 11*, 43−52.
(68) Lee, H. K., Chan, K. F., Hui, C. W., Yim, H. K., Wu, X. W., and Wong, H. N. C. (2005) Use of furans in synthesis of bioactive compounds. *Pure. Appl. Chem. 77*, 139−143.
(69) DeLano, W. L. (2009) PyMOL molecular viewer: Updates and refinements. *Abstracts of Papers*, American Chemical Society, Washington, D.C., *238*.

DOI: 10.1021/acs.biochem.5b00176
Biochemistry 2015, 54, 2997−3008